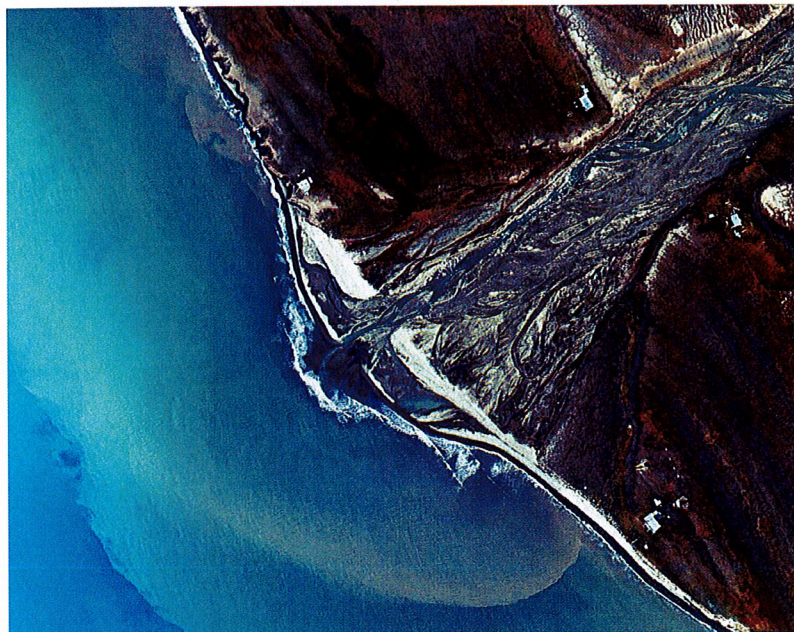


# Physical changes in an Arctic landscape

A multi-decadal case study over Hanaskogdalen,  
Svalbard, Norway using remote sensing



**Siri Holm Hjelmerud**  
**Sofia Persson**

**Degree of Bachelor of Science**  
**with a major in Geography**  
**15 hec**

**Department of Economy and Society, Human Geography &**  
**Department of Earth Sciences**  
**University of Gothenburg**  
**2022 B-1189**

Faculty of Science



UNIVERSITY OF GOTHENBURG

# Physical changes in an Arctic lanscape

A multi-decadal case study over Hanaskogdalen,  
Svalbard, Norway using remote sensing

Siri Holm Hjelmerud  
Sofia Persson

ISSN 1400-3821

**B1189**  
**Bachelor of Science thesis**  
**Göteborg 2022**

## **Abstract**

Local climate change impacts in Arctic regions are of interest for people living in the area, as well as on a global scale to broaden the understanding on how Arctic landscapes are evolving in relation to the Earth's climate system. By conducting a change detection case study using state-of-the-art remote sensing this paper focuses on physical changes in Hanaskogdalen, Svalbard, Norway. Comparing aerial photos from 1936, 1961, 1990, 2008 and 2020 enables identification of observable variations regarding geomorphological activity, coastline development and glacial extension. Furthermore, by using data from the meteorological station SN99840 local climate variations from 1976-2020 are examined. The result of this study indicates multiple physical changes throughout the last decades. Concerning the evolution of the landscape this paper highlights the increase of debris flow occurrences, coastline erosion, delta development at the river mouth and ablation of the glacial snout of Brandtbreen in the eastern part of Hanaskogdalen. Additionally, climate variables have been examined; a positive trend can be found regarding mean annual air temperature, annual precipitation, summer precipitation and days with heavy precipitation. Nevertheless, the only statistically significant change during the period 1976-2020 is the temperature increase.

## **Keywords:**

*Geomorphology, Glacier, Climate, Svalbard, Hanaskogdalen*

## **Sammanfattning**

Konsekvenser av lokala klimatförändringar i arktiska regioner är relevant såväl för boende i området, som på en global skala för att öka förståelsen om hur landskapen förändras i relation till jordens klimatsystem. Via en förändrings-fallstudie så fokuserar denna rapport, med hjälp av fjärranalys, på fysiska förändringar i Hanaskogdalen, Svalbard, Norge. Genom jämförelse av flygbilder från 1936, 1961, 1990, 2008 och 2020 har observerbara förändringar i landskapet identifierats kopplat till geomorfologisk aktivitet, utveckling av kustlinjen och glacial utbredning. Vidare har data från den meteorologiska stationen SN99840 använts för att undersöka det lokala klimatets förändring mellan 1976 och 2020. Studiens resultat visar på flertalet fysiska förändringar i landskapet över de senaste årtionden. Rapporten betonar den ökade mängden slamströmmar, kustlinjens erosion, delta-utvecklingen vid dalens flodmynning och ablationen av Brandtbreen, glaciärstungan i Hanaskogdalens östra del. Därtill har flertalet klimatvariabler undersökts; såväl genomsnittlig årlig lufttemperatur, årlig nederbörd, sommarnederbörd och dagar med kraftig nederbörd påvisar en positiv trend. Dock är det endast temperaturökningen som, av de undersökta variablerna under perioden 1976-2020, statistiskt kan fastställas.

### **Nyckelord:**

*Geomorfologi, Glaciär, Klimat, Svalbard, Hanaskogdalen*

## **Preface**

This bachelor thesis puts an end to 3 years of geography studies at the University of Gothenburg. Initially, when thinking about what our bachelor thesis could be, our common interest in physical geography and remote sensing made us reach out to dr. Andreas Johnsson for inspiration and ideas. He provided us with the knowledge of the new data in need of analysis over Hanaskogdalen, an idea that caught our interest.

We would like to extend our unlimited thanks to our supervisor dr. Andreas Johnsson for being understanding and helpful with every little question we have had. We would also like to thank our course coordinators Sofia Thorsson and Jonas Lindberg, as well as our classmates, for motivation and feedback throughout the process of writing this paper. You have made this experience something special and contributed to the elevation of our study. For support and guidance regarding our statistical analysis, thank you to David Zigiotti. Last, but not least, a big thanks to Deutsches Zentrum für Luft- und Raumfahrt for allowing us to work with their new datasets and Norwegian Polar Institute for access to their data.

Siri Holm Hjelmerud & Sofia Persson, Gothenburg 24-05-2022.

## Table of contents

<b>1. Introduction</b>	<b>1</b>
1.1 Aim	2
1.2 Objectives	2
<b>2. Knowledge overview</b>	<b>3</b>
2.1 Global and local climate change	3
2.2 Processes in periglacial environments	4
2.2.1 Debris flows	4
2.2.2 Permafrost	4
2.2.3 Coastline processes	5
2.2.4 Glaciers and moraines	6
2.3 Remote sensing in change detection studies	6
<b>3. Study area</b>	<b>8</b>
3.1 Climate in the study area	9
<b>4. Method</b>	<b>11</b>
4.1 Remote sensing data & GIS	14
4.2 Climate data & statistical analysis	16
4.3 Discussion of method	17
<b>5. Results</b>	<b>20</b>
5.1 Geomorphological change	23
5.2 Glacial change	26
5.3 Climate change	28
<b>6. Discussion</b>	<b>32</b>
6.1 Impacts on society	34
<b>7. Conclusion</b>	<b>36</b>
<b>8. References</b>	<b>37</b>

# 1. Introduction

The warming climate affects all parts of the world in various ways and at different rates. However, climate change impacts in Arctic regions are disproportionately large with consequences including increased temperatures, changed precipitation patterns and elevated sea level (Anisimov et al., 2007). A greater understanding of how climate change is disturbing Arctic regions is of interest at a global and local scale. In a global perspective, variations in Arctic regions must be considered in relation to the Earth's climate system, and climate change feedbacks needs to be taken into account. The changed albedo by melting glaciers and the potential methane and carbon dioxide emissions from degradation of organic material due to the thawing of permafrost both pose a threat to further accelerate global warming (Mason, Burt, Muller & de Blij, 2016, p. 232; Song et al., 2020). On a local scale, people in Svalbard, Norway already have to alter their way of living to adapt to climate change impacts (Timlin, Meyer, Nordström & Rautio, 2022). Furthermore, it must be recognized that in the future these may accelerate and new challenges may occur.

Due to an interest in investigating these areas the Deutsches Zentrum für Luft- und Raumfahrt (DLR) obtained high resolution aerial photographs over the Arctic and Antarctica in 2008 and 2020 (DLR, 2010; DLR, n.d.). In 2008 several regions in Svalbard were covered by this new flight campaign aiming to obtain aerial images in high detail of these unique environments (DLR, 2010). This was complemented in 2020 with new photographs in even greater detail (DLR, n.d.). Historically, the Norwegian Polar Institute (NPI) has obtained data over the same areas (Geyman, van Pelt, Maloof, Aas & Kohler, 2021) which provides a multi-decadal coverage of aerial data and allows for a detailed change detection case study over the landscape. The newly obtained and unanalyzed data enables a study of physical changes that have occurred over an extensive period of time, which can be beneficial for gaining awareness on potential future changes that could be prepared for. Increasing the knowledge of landscape variations in the Arctic is of relevance for people living in the region, but also in similar regions and for the planet as a whole considering in the Earth's climate system.

Previous studies have connected geomorphological activity in Svalbard with a changed climate (de Haas, Kleinhans, Carbonneau, Rubensdotter & Hauber, 2015) and examined debris flows recurrence and magnitude in detail on one specific alluvial fan in the valley Hanaskogdalen, Svalbard from 1961 to 2013 (Bernhardt, Reiss, Heisinger, Hauber & Johnsson, 2017). To

complement these studies a broader perspective, covering the entire valley over a prolonged timespan and including other detectable physical changes, could provide further insights.

### ***1.1 Aim***

This multi-decadal case study seeks to detect physical changes in the Arctic landscape of Hanaskogdalen, Svalbard, Norway to determine what effects global warming has on these environments. Geomorphological and glacial variations will be observed at five different points in time during the period 1936-2020 while climate variables, precipitation and temperature change, will be investigated between 1976-2020.

In order to fulfill the aim state-of-the-art remote sensing and statistical analysis will be the primary methods. A change detection study will be executed, and the most distinct landscape changes investigated by quantifying the results and discussing what processes might have caused these variations.

### ***1.2 Objectives***

- What geomorphological and glacial changes are visual when comparing aerial photos over Hanaskogdalen in Svalbard between the years 1936, 1961, 1990, 2008 and 2020?
- Regarding local climate, how has temperature and precipitation changed in the area from 1976-2020?

## **2. Knowledge overview**

### ***2.1 Global and local climate change***

Human actions and emissions are altering the composition of the atmosphere, escalating greenhouse gas concentration leading to an increased air and sea surface temperature (Mason et al., 2016, p. 243 & 250-251). The Intergovernmental Panel of Climate Change (IPCC) (2018a) highlights the fact that impacts from a changed climate are already visual and for every degree of warming the reactions will be more distinct. The global trends are that the mean air temperature is going to increase and that precipitation patterns will change. The high latitudes in the Northern hemisphere are projected to see an increase in temperature, precipitation and heavy precipitation (IPCC, 2018b). Looking at the Earth's climate system possible feedbacks must be considered; a positive feedback is enhancing while a negative counteracts the initiative change (Mason et al., 2016, p. 8; Steffen, Rockström, Richardson & Schellnhuber, 2018). For example, ice-albedo feedback occurs when higher temperatures intensifies melting of snow and glaciers, altering albedo and increasing solar radiation absorption which enhances temperatures (Mason et al., 2016, p. 232).

Regarding the climate in Svalbard, IPCC (2018b) projects that the climate change impacts are going to be disproportionately high compared to the global mean. There is a somewhat disagreement in previous studies regarding the significance of the already observed precipitation and temperature changes in Svalbard. Hanssen-Bauer and Førland (1998) found that annual precipitation displayed a 30% increase between 1912 and 1996 and throughout this timespan the annual precipitation and summer precipitation shows statistical significance. In 2003 the significance throughout the 20th century was confirmed by Førland and Hanssen-Bauer (2003). In contrast, Bernhardt et al. (2017) could not establish statistical significance looking at summer precipitation or mean annual air temperature change from 1961 to 2013. Regarding temperature, Hanssen-Bauer (2002) supports this when looking at temperature change between 1912 and 2020, however Jörpeland (2014) contradicts by finding a significant increase regarding mean annual air temperature between 1989 and 2010.

## ***2.2 Processes in periglacial environments***

### **2.2.1 Debris flows**

Debris flows are defined as masses of sediment often saturated with water surging downhill creating levees on the side, figure 1, resulting in an accumulation of sediment in the formation of a fan (French, 2007, p. 233).



*Figure 1 - Debris flow in Hanaskogdalen, Svalbard. Photographed 13.08.2013. Source: Bernhardt et al. (2017).*

*Figur 1 - Slamström i Hanaskogdalen, Svalbard. Fotograferad 13.08.2013. Källa: Bernhardt et al. (2017).*

In Arctic regions debris flows are a common phenomena that can possibly have a large impact on geomorphology and human everyday life (Bernhardt et al., 2017). In Svalbard, frost weathering provides the slopes with sediment of various sizes which, together with water saturation, is beneficial for triggering debris flows (de Haas et al., 2015). The major reason for triggered debris flows in the region is heavy rainfall (Bernhardt et al., 2017), however there is a discussion among researchers of the impact which fast melting snow can have on geomorphological movements (Bernhardt et al., 2017; de Haas et al., 2015; McCann, Howarth & Cogley, 1972).

### **2.2.2 Permafrost**

In periglacial environments permafrost is an important phenomena to consider. The definition of permafrost is ground remaining at or below 0°C for two or more consecutive years (Howard et al., 2022). In the active layer, the upper part of the ground that freezes and thaws annually,

precipitation can cause saturation since the permafrost below inhibits water infiltration (Mason et al., 2016, p. 556). A frozen ground can have a stabilizing effect which is why the geomorphological movement is limited to the active layer when the ground is not frozen or snow covered (de Haas et al., 2015; Guerra, Fullen, Jorge, Bezerra & Shokr, 2017). A changing climate can therefore affect geomorphological activity since increased temperature causes thawing of permafrost, but also changes the precipitation from snow- to rainfall (Howard et al., 2022; Tananaev & Lotsari, 2022). Furthermore, de Haas et al. (2015) concludes that on a local scale activity on alluvial fans in Svalbard is likely to accelerate due to increased temperature and amount of rain. Bernhardt et al. (2017) have used remote sensing and in situ studies to examine changes of debris flows on one of the larger alluvial fans in Hanaskogdalen from 1961 to 2013, and states that recurrence and magnitude has increased.

### 2.2.3 Coastline processes

The development of a coastline is a complex process primarily defined by hydrological mechanisms. In periglacial environments the main contributors to coastline erosion is frost weathering, wave action and thermal erosion (Ballantyne & Harris, 1994, p. 271; Dupeyrat et al., 2011). On a global scale a rise in sea level can be attributed to the increased temperature both through thermal expansion and the melting of glaciers (National Aeronautics and Space Administration [NASA], 2022). A higher sea level can affect the development of the coastline, exposing new surfaces to eroding processes (Ballantyne & Harris, 1994, p. 267). At a river mouth a delta can develop in various shapes and sizes, figure 2, and the formation is affected by the river's discharge and the amount of sediment it transports, as well as the strength of currents, waves and tides (Mason et al., 2016, p. 504).

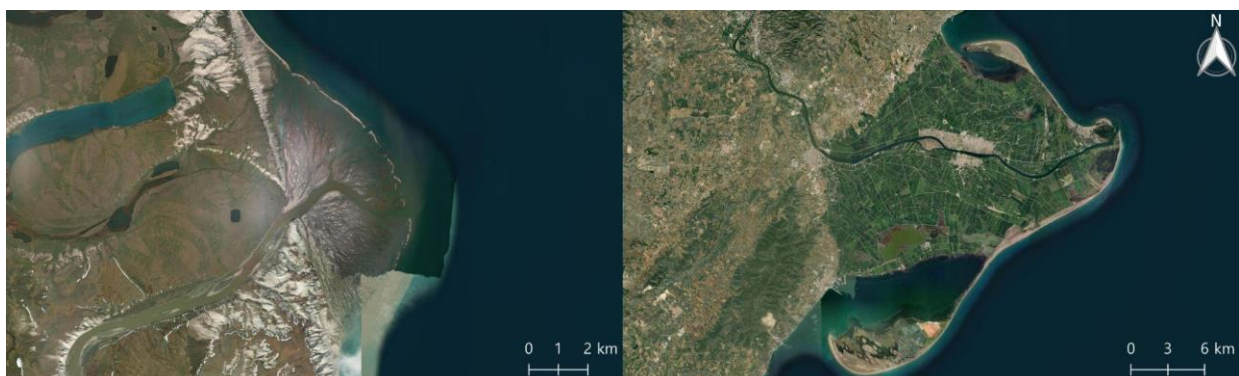


Figure 2 - Example of different types of delta formations. The river outlet of the Horton river in Canada (left) and Ebro river in Spain (right). Source: Authors own. Data source: ESRI.

Figur 2 - Exempel på olika typer delta formationer. Älvmynningen av Horton älven i Kanada (vänster) och Ebro älven i Spanien (höger). Källa: Författarnas egna. Datakälla: ESRI.

Fluvial systems in periglacial environments are regulated by the amount of snowmelt and rainfall (Beylich & Gintz, 2004). Sediment transport is greatest during runoff peaks and therefore the amount of discharge is relevant to consider (ibid). The sediment can later be deposited to create a river delta (Mason et al., 2016, p. 504).

#### **2.2.4 Glaciers and moraines**

As a glacier moves it can transport material and shape the landscape underneath it, resulting in landforms visible when the glacier retreats (National Snow & Ice Data Center [NSIDC], 2020). The most distinct glacial depositional landform is the moraine which can form through different processes. Sediment can fall down onto the glacier or be pushed in front creating a build up (Ibid). When the glacier is at maximum extent a terminal moraine is created (Mason et al., 2016, p. 539). Air temperature influences a glacier primarily since a warmer climate causes retreat, but also affects erosion and movement (ibid, p. 527). The glacier is divided into two parts; the accumulation zone where new snow is becoming a part of the glacier and the ablation zone where the major melting occurs and ice mass is lost (ibid, p. 524). If the accumulation and ablation happens simultaneously and at the same rate the system is at equilibrium, making the mass balance neutral and the glacier neither grows nor shrinks (ibid, p. 524-525). On a global scale research shows a decrease of glaciers at an accelerating speed (World glacier monitoring service [WGMS], 2021). Regarding Svalbard the same trend is observed (ibid). Earlier studies in Svalbard have stated that areas of previous glaciation tend to be more unstable and prone to geomorphological movement; so called paraglacial activity (de Haas et al., 2015).

### ***2.3 Remote sensing in change detection studies***

Remote sensing can be used for Earth observations to effectively monitor large regions and detect changes in areas without physically having to be there (Harrie, 2013, p. 115). Obtaining remote sensing data can be done using multiple sensors that are divided into two main categories; active and passive. Aerial photos are obtained using a passive sensor, meaning that it registers how different surfaces absorb or reflect sunlight in different wavelengths called an object's spectral signature (ibid, p. 116). The different wavelengths can be visualized in different combinations depending on purpose. Combining wavelengths *red*, *green* and *blue* (RGB) allows for creation of images in *true color*; as the human eye would see it (ibid, p. 117-118). With the *near infrared* (NIR) wavelength one can create a *false color IR* visualization,

which is primarily used for vegetation monitoring since the NIR wavelength reflects chlorophyll (ibid, p. 117-118). Certain land covers such as water and snow have particular spectral signatures. Water absorbs energy in all wavelengths and thereby it appears dark, while snow reflects the majority resulting in a light color (European Space Agency [ESA], n.d.; Jones & Vaughan, 2010, p. 47).

### 3. Study area

The area for this study is Hanaskogdalen, a valley in Svalbard, Norway, figure 3, and throughout this section the physical and climatic features of the area will be presented.

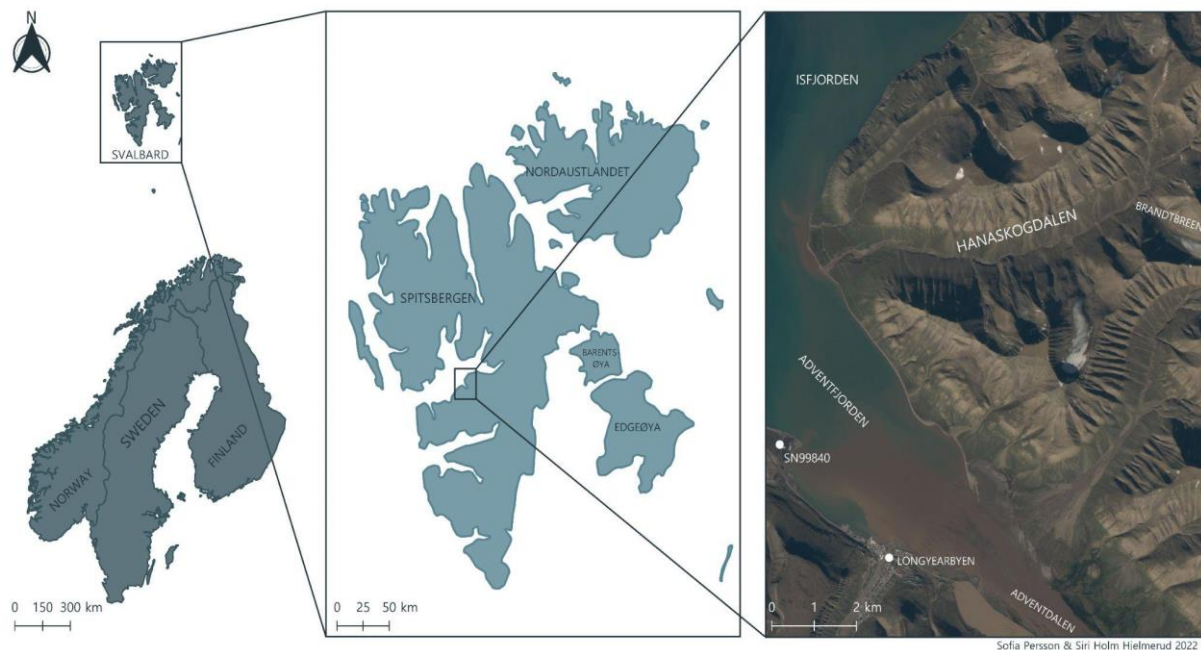


Figure 3 - The location of Hanaskogdalen in Svalbard, Norway. Source: Authors own (2022).

Data source: ArcGIS Hub and NPI (EPSG:3995).

Figur 3 - Hanaskogdalens placering i Svalbard, Norge.

Källa: Författarens egna (2022). Datakälla: ArcGIS Hub och NPI (EPSG:3995).

Svalbard is a group of islands, residing between latitude 74°N and 81°N, which are characterized by glaciers, mountains and fjords (Thuesen & Barr, 2022). The study area for this paper is located on the largest island, Spitsbergen, which has a variation in topography with valleys separating large mountain massifs (Hauber et al., 2011). The number of habitants in Svalbard is approximately 3000 with the majority living in Longyearbyen, the administrative center (Thuesen & Barr, 2022). It has been referred to as a paradise for geologists since all geological systems are represented, from pre-Cambrian to present Quaternary (Sollid & Christiansen, 2003, p. 1). The soil is classified as leptic cryosols; a permafrost soil developed over a rocky foundation (Hauber et al., 2011). The permafrost is approximately between 100 and 500 meters thick with the thinner layer residing at lower altitudes (Sollid & Christiansen, 2003, p. 13).

Hanaskogdalen is situated on latitude 78°N, just north of Longyearbyen, figure 3. It is a U-shaped valley that is approximately 10 km long and 2,5 km wide (Bernhardt et al., 2017). The valley is located in a periglacial environment, an environment on the perimeter of glaciation (Mason et al., 2016, p. 555), and characterized by coalescing alluvial fans along the valley walls and the glacial snout of Brandtbreen, a valley glacier, in the eastern part. There is a small river running in the middle of the valley with the river outlet in Adventfjorden. Opposite the river mouth, at Svalbard Airport approximately 3 km southwest of the study area, the closest meteorological station is located, SN99840.

The choice of study area was determined by the disproportionately large climate impacts in Arctic regions, the newly gathered and previously unstudied data over the area as well as the vast amount of aerial photos dating back to 1936. Furthermore, the study area is of interest due to its proximity to Longyearbyen as the knowledge obtained by this study has the possibility to be applied there.

### ***3.1 Climate in the study area***

In Arctic regions the climate change is rapid and the consequences vary from loss of glaciers to rise in sea level and permafrost thaw (IPCC, 2018b). Svalbard is among the most affected by climate change in the Arctic, especially concerning the air temperature during winter. Annual air temperature has increased during the last decades and continuing to the end of the century winter air temperature is expected to be approximately 10°C higher than today (Timlin et al., 2022).

The meteorological stations at Spitsbergen, Svalbard have at least one month of mean air temperature above 0°C yearly indicating a *tundra climate* (ET) according to the Köppen classification (Climate change & infectious diseases group, 2019; Sollid & Christiansen, 2003, p. 47). The average temperature between 2010 and 2020 was -2,6°C, and average annual precipitation 221 mm (Norsk Klimaservicesenter, n.d.). Throughout the year there is a variation in solar radiation impact in the area (Sollid & Christiansen, 2003, p. 47). During summer the midnight sun provides 3-4 months with continuous daylight, in contrast to winter when the area experiences total darkness for 3-4 months. In summer net radiative heat is limited because of the low sun angle and reflectivity of the snow regardless of the midnight sun (ibid, p. 47).

An understanding of local snow coverage is of relevance due to the possible effects on geomorphological processes. There is an indication of changes in the thawing of snow in Svalbard; generally it is initiated at the end of June however observations show a trend in earlier melting (Norwegian Meteorological Institute, 2021). Furthermore, despite the annual variation, studies show an enhancement of the area that becomes snow free during summer as well as lesser sea-ice in the surrounding ocean (ibid). Another aspect of geomorphological activity is that the ground stability is affected by permafrost, which has been monitored in Adventdalen since 1998 (Norwegian Meteorological Institute, n.d.). These observations show a variation in ground temperature throughout the year with a temperature peak in August and September (ibid). There is also an annual fluctuation with a trend that shows an increase of temperature throughout the permafrost profile. Studies show a correlation between ground surface temperature and air temperature partly due to the sparse vegetation in the area (ibid).

## **4. Method**

This change detection study was conducted through remote sensing with aerial photos from 1936, 1961, 1990, 2008 and 2020. A comparison of the images enabled identification and mapping of observable changes throughout the period. Furthermore, a climate data analysis was conducted to increase the knowledge on precipitation and temperature changes in the area over the last decades.

The observed physical changes were categorized to allow for comparison on the amount of changes in different time periods. When mapping new debris flows our method was based on previously similar studies (Bernhardt et al., 2017). Figure 4 illustrates an example of the process of mapping physical changes, in this case debris flows, comparing aerial photos and hillshades from different years. Although the study area is sparsely vegetated, the NIR-data can be used to identify lichen growth to detect debris flow activity (ibid). Previous studies have been conducted partly based on the field study method of lichenometry (ibid). However, this study primarily used lichen as an indicator of occurrence of debris flows as these disturb the landscape leaving un-vegetated channels detectable in the *false color IR* visualization.

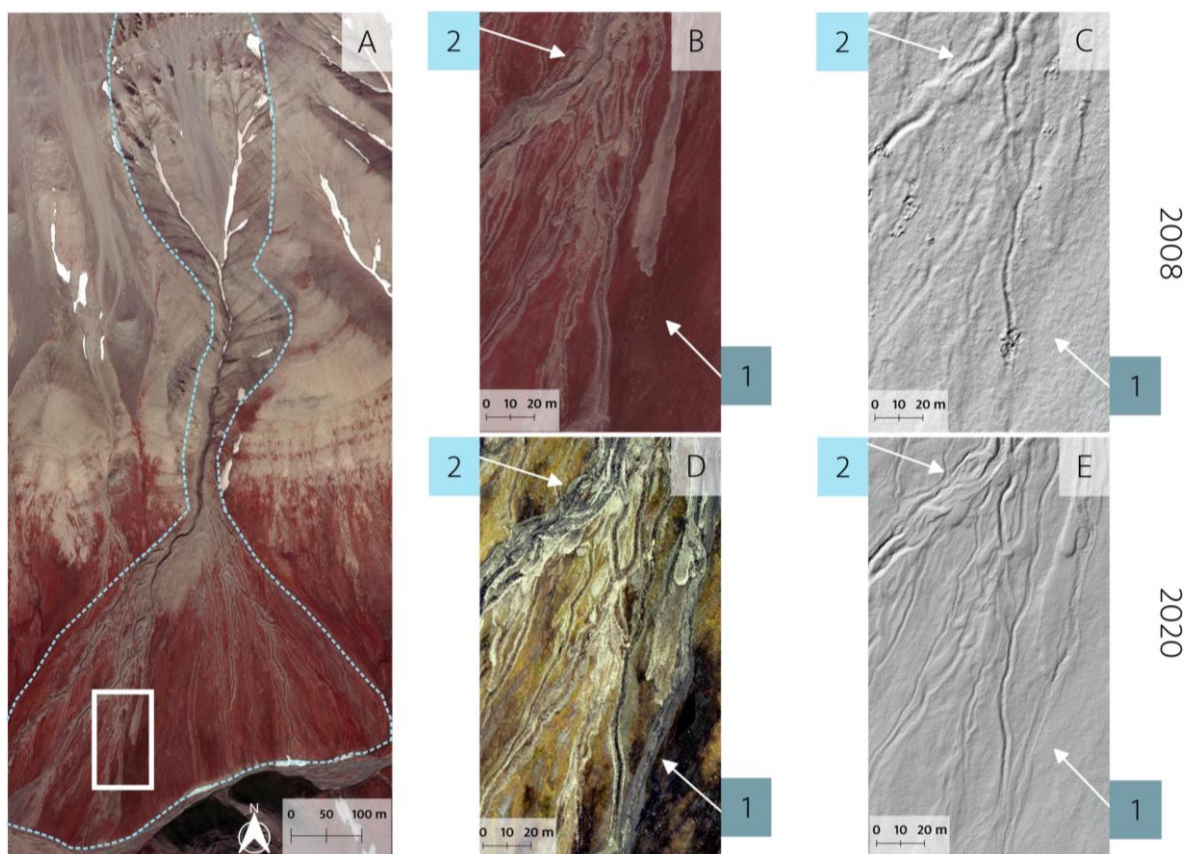
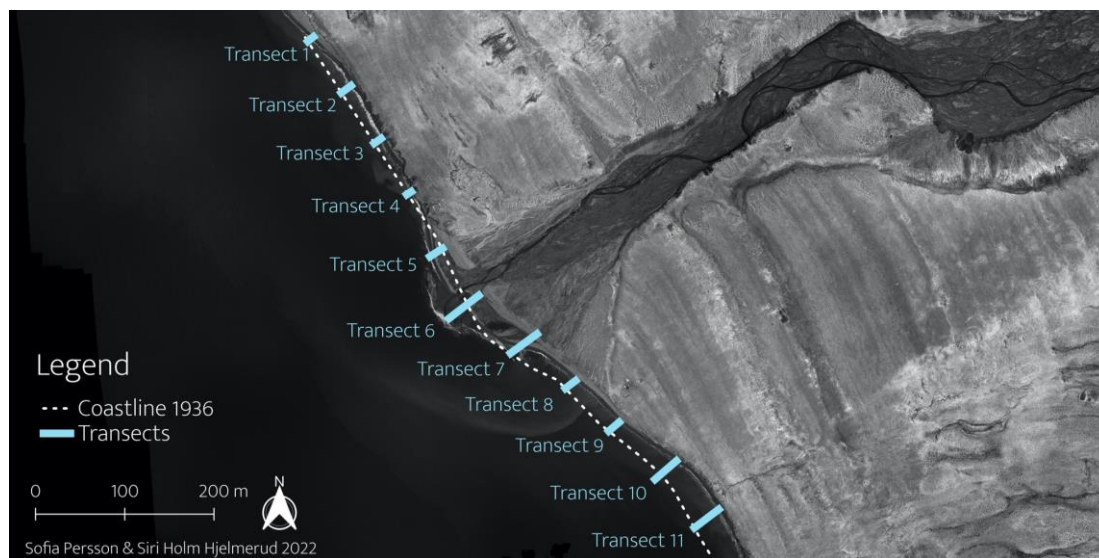


Figure 4 - Example of method used when detecting change in the study area. The blue dots outline the alluvial fan (A) and the zoomed in area is marked. (B) and (C) are from 2008; false color IR visualization and hillshade respectively. (D) and (E) are from 2020 and are true color and hillshade. (1) and (2) are pointing out activity of debris flows that can be detected when comparing the different years. Source: Authors own (2022). Data source: DLR (EPSG:3995).

Figur 4 - Exempel av metoden använd för att upptäcka förändringar i området. Det blåa strecket visar ytterkanten av alluvialkonen (A) och markeringen visar området de andra kartorna är inzoomade på. De blå (B) och (C) är från 2008; falsk färg IR-visualisering och terrängskuggning. (D) och (E) är från 2020 och är äkta färg och terrängskuggning. (1) och (2) pekar ut slamströms-aktivitet som kan observeras vid jämförelse mellan de två åren. Källa: Författarnas egna (2022). Datakälla: DLR (EPSG:3995).

There is one km of coastline covered by the aerial images from 1936, 1990, 2008 and 2020, and this stretch is the area of examination regarding coastline development. To be able to quantify the results 11 transects were evenly spaced along the coastline, figure 5. 1936 served as the reference line from which the other years were compared to.



*Figure 5 - The distribution of Transects along the coastline, at which the coastline in 1990, 2008 and 2020 was measured and compared to the reference which was 1936. The transects are placed 100 m apart.*

*Source: Authors own (2022). Data source: DLR (EPSG:3995).*

*Figur 5 - Fördelningen av tvärsnitt längst kustlinjen, vid vilka kustlinjerna år 1990, 2008 och 2020 mättes mot referenspunkten 1936. Tvärsnitten är placerade 100 m ifrån varandra. Källa: Författarens egna (2022).*

*Datakälla: DLR (EPSG:3995)*

Considering glacial change the extent was digitized at the different years allowing for area calculation and comparison. Therefore it is possible to identify if the glacier has advanced or retreated.

#### 4.1 Remote sensing data & GIS

The software used to execute the remote sensing analyzes was QGIS. The choice of software was primarily determined by the fact that it contains relevant tools, availability and our previous knowledge and experience of working with remote sensing in the program. All data used in these analyzes are listed in table 1 below.

Table 1 - Datasets used to conduct remote sensing analyzes, with format, source, resolution and sensor.

Tabell 1- Data använd för att genomföra fjärranalyser, inklusive format, källa, upplösning och sensor.

Dataset	Format	Source	Resolution (m)	Sensor
World map	Vector	ArcGIS Hub	-	-
Svalbard Orthophoto	Raster	NPI	0.16	-
Svalbard Orthophoto 1936 ( <i>gray</i> )	Raster	Geyman et al. (2021)	20	Aerial
1961, 15 <sup>th</sup> of August ( <i>gray</i> )	Raster	NPI	1	Aerial
1990, 22 <sup>th</sup> of July ( <i>false-color infrared</i> )	Raster	NPI	1	Aerial
Svalbard Aerial photo ( <i>false-color infrared</i> ) 2008, 23 <sup>th</sup> of July	Raster	DLR	0,2	HRSC-AX
DEM 2008	Raster	DLR	0,5	HRSC-AX
Hanaskogdalen Aerial photo 2020 ( <i>true color</i> )	Raster	DLR	0,1	MACS-polar
Hanaskogdalen Aerial photo 2020 ( <i>near infrared</i> )	Raster	DLR	0,1	MACS-polar
DEM 2020	Raster	DLR	0,1	MACS-polar

The aerial photos were acquired with different sensors that can intercept radiation at various wavelengths resulting in variations among the data (Harrie, 2013, p. 116). The data from 1936 is an aerial photograph from the NPI's collection of photos capturing Svalbard in 1936/1938,

which have been georeferenced in Metashape using ground control points (Geyman et al., 2021). The aerial photo is in single band (*grey*) visualization. The data from 1961 and 1990 are also aerial photographs collected by the NPI; the 1961 data in single band (*grey*) visualization, and the data from 1990 in *false color IR*. For 2008 the sensor used was an airborne HRSC (High Resolution Stereo Camera)-AX camera (DLR, 2010) while for 2020 the MACS (Modular Aerial Camera System) polar aerial camera was used (DLR, n.d.). The datasets from the years 2008 and 2020 acquire images in visual RGB and NIR wavelengths (DLR, 2010; DLR, n.d.). The aerial photos were obtained using a passive sensor. The unique spectral signatures of water and ice enable identification of these land covers even on older photos with poorer resolution, allowing a change detection study of glacial expansion and evolution of coastline, figure 6.

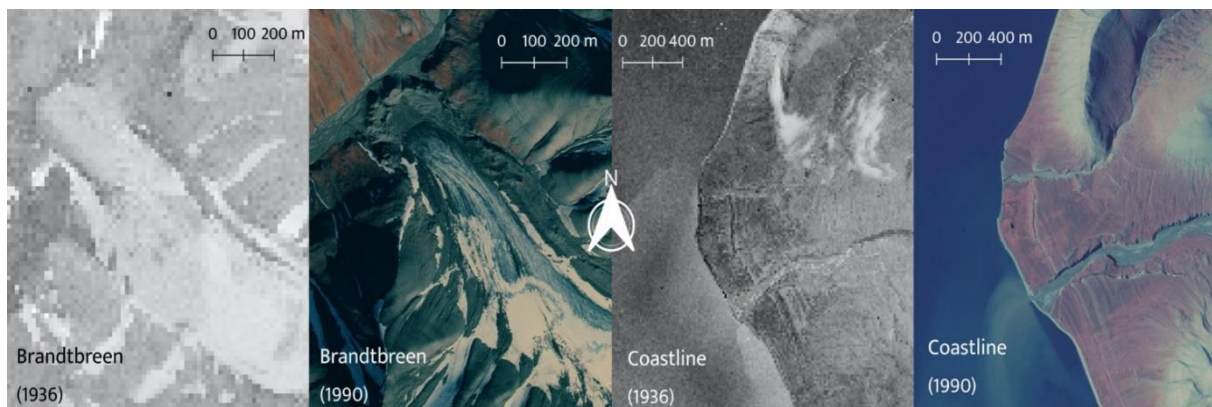


*Figure 6 - The glacier Brandtbreen and the coastline 1936 and 1990, displaying how the unique spectral signatures makes it possible to identify glaciers and water on photos with lesser resolution.*

*Source: Authors own (2022). Data source: NPI & Geyman et al. (2021) (EPSG:3995)*

*Figur 6 - Glaciären Brandtbreen och kustlinjen 1936 och 1990, visar hur de unika spektrala signaturerna av vatten och is möjliggör identifiering och kartering, även på äldre, mindre upplösta bilder.*

*Källa: Författarnas egna (2022). Datakälla: NPI & Geyman et al. (2021) (EPSG:3995).*

A few of the aerial photos from 1961 and 1990 were not georeferenced when received so to enable inclusion in the analyzes they had to be, using the 2008-data as reference. The control points, which were for example ridges and alluvial fans, were mainly focused around Hanaskogdalen since the area of interest should be the best covered to get a good result (Harrie, 2013, p. 193). There was a slight displacement after the georeferencing which needed consideration throughout the analyzes.

## ***4.2 Climate data & statistical analysis***

For the purpose of investigating how the local climate has changed in the study area throughout the last decades, data from Norsk Klimaservicesenter was used. Considering that temperature and precipitation are the primary factors affecting geomorphological, glacial, and hydrological processes in the area (de Haas et al., 2015) the climate analysis was limited to these variables. The climate data ranged from 1976 to 2020 and was collected at Svalbard Airport weather station, SN99840, right across Adventfjorden from the study area.

By using Excel and Stata the climate data was analyzed and a regression analysis was made. The bivariate regression model was used to predict the relation between time and climate variables. The  $\beta$ -coefficient is of interest in the regression analysis since it shows the independent variable's effect on the dependent variable (Cortinhas & Black, 2012, p. 493). The  $R^2$  value shows the percentage of variation in the dependent variable that is explained by the independent variable (ibid, p. 562). Regarding scientific significance the p-value to indicate significance is considered to be 0.05.

Time was set as the independent variable. The dependent variables being examined were mean annual air temperature, total annual precipitation, amount of precipitation between June 15<sup>th</sup> and September 15<sup>th</sup> when minimum temperature was over 0°C and number of days with heavy precipitation (more than 5 mm) between 15<sup>th</sup> of June and 15<sup>th</sup> of September when minimum temperature was above 0°C. Forward, amount of precipitation between June 15<sup>th</sup> and September 15<sup>th</sup> when the minimum temperature was over 0°C will be referred to as *summer precipitation*, and the number of days with heavy precipitation (more than 5 mm) between 15<sup>th</sup> of June and 15<sup>th</sup> of September when minimum temperature was above 0°C as *days with heavy precipitation*. Restraining the precipitation to summer months and temperatures above 0°C is because the purpose is to evaluate rain that has fallen on snow free ground. As previously mentioned, due to the fact that the region is sparsely vegetated there is a correlation between surface temperature and air temperature (Norwegian Meteorological Institute, n.d.). Additionally, this definition is used in previous studies by Bernhardt et al. (2017) and strengthened by research on snow accumulation and melting throughout the year in Svalbard (Norwegian Meteorological Institute, 2021). Regarding mean annual air temperature and total annual precipitation the data was collected per year while the other two precipitation variables were collected per day to enable exclusion of days with minimum temperature below 0°C.

### 4.3 Discussion of method

When using remote sensing it is of importance to consider that one of the main benefits with the method, the possibility to collect and analyze data in areas without visiting them, also can be regarded as a flaw. Since the foundation is interpretation there is an inherited risk for subjectivity. Furthermore, there is a need to mention the variation between the photos. When analyzing data from various instruments and years the spectral resolution can vary and thereby alter the result (Harrie, 2013, p. 119). To minimize misinterpretation due to subjectivity and variation in resolution the images were studied both from newest to oldest and oldest to newest. The time of day and year of capture may result in differences in regards to vegetation, shades, cloud and snow cover which had to be considered during the analyzes. The slight displacement of the georeferenced data made the change detection difficult and consideration had to be made throughout the study. The data from 1961 did not cover the entire study area, therefore there is a larger gap in the data covering the river outlet and coastline. A shortened gap between observation points could provide additional data that would benefit the study. However, as already discussed by Bernhardt et al. (2017), images from sensors such as Landsat or SPOT would not be beneficial because of the resolution ( $>10\text{m}/\text{px}$ ) that would be considerably poorer than the aerial photos used. Availability was also the reason why satellite photos could not complement the lacking coverage of the 1961 data.

Figure 7 shows the difficulties connected to using data from different years. The resolution of the 1936 image makes it impossible to detect smaller changes such as fluvial changes or new debris flows. Additionally the figure illustrates the variation of snow and shadows between the years which possibly could affect the result.

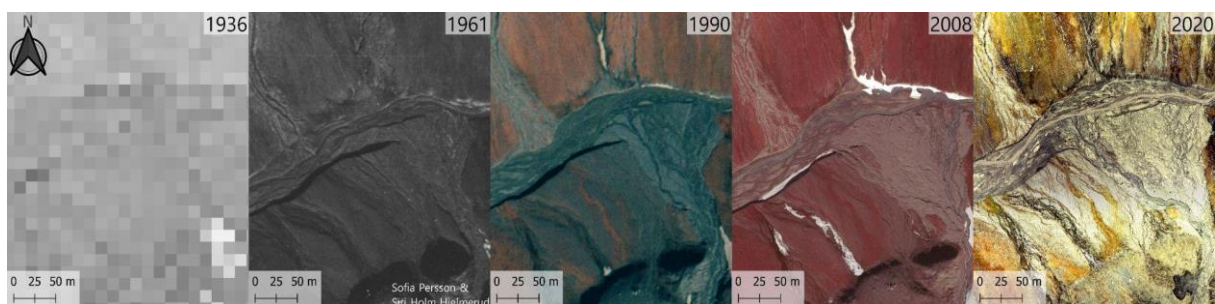


Figure 7 - The same area in the different years, makes the differences in resolution, snow coverage, shadows and visual spectrum noticeable. Source: Authors own (2022). Data source: NPI, Geyman et al., (2021) & DLR (EPSG:3995).

Figur 7 - Samma område under de olika åren, gör skillnader i upplösning, snötäckte, skuggning och visuellt spektrum tydliga. Källa: Författarnas egna (2022). Datakälla: NPI, Geyman et al., (2021) & DLR (EPSG:3995).

Considering the climate data the precipitation range and the timespan can be discussed. As previously mentioned precipitation fallen between 15<sup>th</sup> of June and 15<sup>th</sup> of September when the minimum temperature was above 0°C was chosen due to the purpose of solely looking at rainfall on snow free ground. However, there is a possibility of precipitation falling as snow within these dates and temperature limit. Nevertheless, the definition has been used in previous studies (Bernhardt et al., 2017) which supports the choice made. Regarding timespan a more extensive period of time could be beneficial, but that would require interpolation from other meteorological stations which would deprive the study of the local perspective.



## **5. Results**

Throughout this study multiple changes have been identified in the study area regarding geomorphological, glacial and climate variations which will be presented in this segment.

Concerning geomorphological and glacial changes there is a variation in the amount of detected observable landscape alterations throughout the years, figure 8. The resolution of the 1936 data complicates detection of smaller changes, however glacial development and coastline evolution are observable from 1936 to 2020. Nevertheless, since the coverage of the 1961 data was deficient and not covering the coast, the coastline change is detectable between 1936 and 1990, map B in figure 8. This is also the reason why there are no changes detected in the western part of map C, figure 8. The majority of changes are detected between 2008 and 2020 as seen in map E, figure 8. Erosion and accumulation of sediment was detected in the floodplain and throughout the coastline. The fluvial changes detected are changes in meandering of the river.



Sofia Persson & Siri Holm Hjelmerud 2022

Figure 8 - The detected changes in different time spans; (A) displays the changes during the entire period (1936-2020), and (B), (C), (D) and (E) are focused on changes between two different years.

Source: Authors own (2022). Data source: NPI, Geyman et al., (2021) & DLR (EPSG:3995).

Figur 8 - De observerade skillnaderna mellan de olika tidsperioderna; (A) visar skillnaderna över hela perioden, och (B), (C), (D) och (E) fokuserar på skillnader mellan två olika år.

Källa: Författarnas egna (2022). Datakälla: NPI, Geyman et al., (2021) & DLR (EPSG:3995).

Figure 9 visualizes the absolute number of observed changes shown in figure 8. More changes have occurred between 2008 and 2020 than the other timespans, except for glacial change where only one point was placed regardless of how distinct the ablation was. A larger number of new debris flows have been detected between 1961-1990 than 1990-2008. However, it is worth mentioning that the length of each timespan varies and this diagram shows the absolute, not the relative, number of changes. An increased number of observations have been detected regarding accumulation of sediment, erosion and fluvial changes as well.

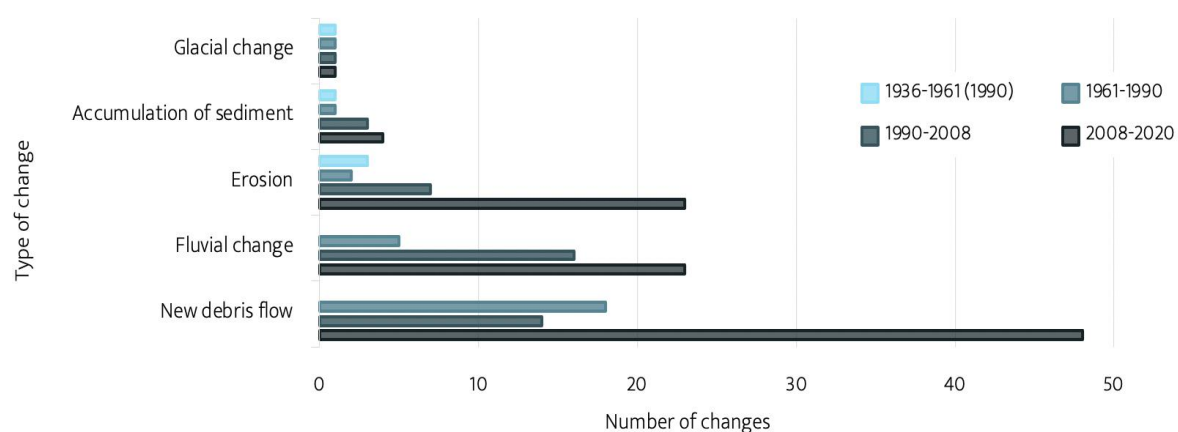


Figure 9 - A staple diagram of the absolute number of changes observed in the different timespans.

Source: Authors own (2022).

Figur 9 - Stapeldiagram av det absoluta antalet observerade skillnader i de olika tidsspnnen.

Källa: Författarnas egna (2022).

## 5.1 Geomorphological change

The main geomorphological changes identified are new debris flows and the changed coastline. Concerning debris flows it is observable that new flows have appeared primarily between 2008 and 2020. New debris flows are possible to identify on multiple alluvial fans in the valley, but particularly on larger fans, figure 10. The debris flows are relatively evenly spatially distributed along the valley walls, however there is a decline in the number of observed new debris flows closer to the coastline.

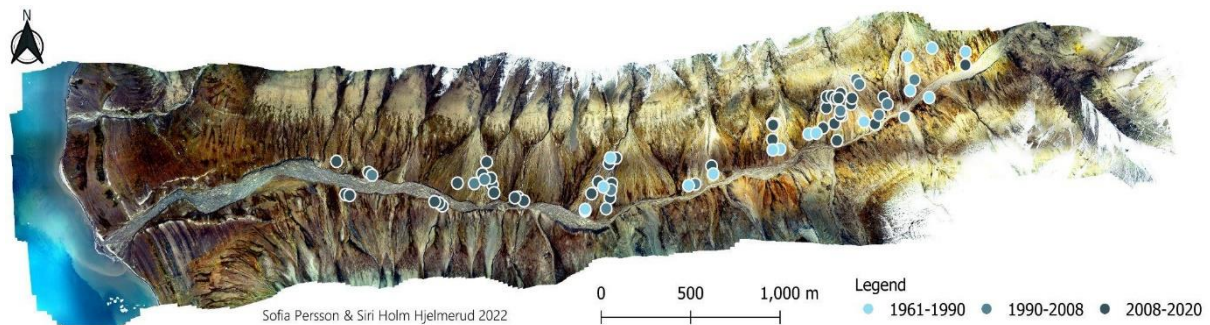


Figure 10 - The different amounts of observed debris flows in the time spans 1961-1990, 1990-2008 and 2008-2020. Source: Authors own (2022). Data source: DLR (EPSG:3995).

Figur 10 - Det olika antalet observerade slamströmmar i tidsspnnen 1961-1990, 1990-2008 och 2008-2020. Källa: Författarnas egna (2022). Datakälla: DLR (EPSG:3995).

There is a clear increase when looking at the relative number of occurring debris flows per year, figure 11. Between 1961 and 1990 the average number of new debris flows per year was  $\sim 0,62$ , while between 1990 and 2008 it was  $\sim 0,78$ . The latest period (2008-2020) shows a considerable increase,  $\sim 4$  new debris flows per year was detected on average indicating a positive trend.

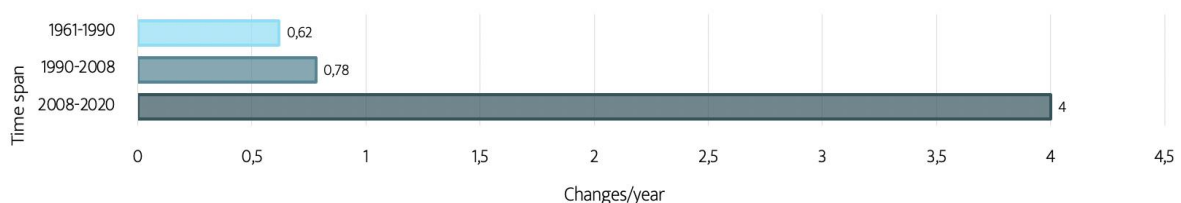


Figure 11 - The average yearly amount of debris flows within the different timespans.

Source: Authors own (2022).

Figur 11 - Årliga medelvärdet på antal slamströmmar inom de olika tidsspnnen.

Källa: Författarnas egna (2022).

Regarding the coastline there is an identifiable change from 1936 until 2020. Along the coastline variations have appeared at different periods. It is possible to detect degradation as well as accumulation of sediment, figure 12. The most distinct accumulation of sediment is between 2008 and 2020 at the river mouth, and at the southernmost part of the coastline erosion can be detected between all years.



*Figure 12 - The variation in the coastline 1936, 1990, 2008 and 2020.*

*Source: Authors own (2022). Data source: Geyman et al. (2021), NPI & DLR (EPSG:3995).*

*Figur 12 - Kustlinjens variation år 1936, 1990, 2008 och 2020.*

*Källa: Författarnas egna (2022). Datakälla: Geyman et al. (2021), NPI & DLR (EPSG:3995).*

The variation along the coastline is visualized in figure 13. The most conspicuous changes are the degradation that has appeared since 1936 at *Transect 9-11* and the aggradation of sediment between 2008 and 2020 at *Transect 5* and *Transect 6*. At *Transect 11* the coastline retracted with 19,9 m between 1936 and 1990, 6,9 m between 1990 and 2008 and 7,7 m between 2008 and 2020. In total, the degradation was 34,5 m from 1936 to 2020. *Transect 6*, located at the river mouth, shows a retraction between 1936 and 2008 but an aggradation between 2008 and 2020. This indicates that the coastline during the 11 years between 2008 and 2020 have advanced from -16,8 m to +26,1 m, an advancement of 42,9 m in total. There is an accumulation of sediment at *Transect 5* between 1936 and 1990 as well, which appears to have been eroded until 2008. Generally it can be said that the majority of the coastline, except the previously mentioned accumulation, has degraded since 1936. More degradation has occurred on the southern side of the river mouth (*Transect ID* > 7).

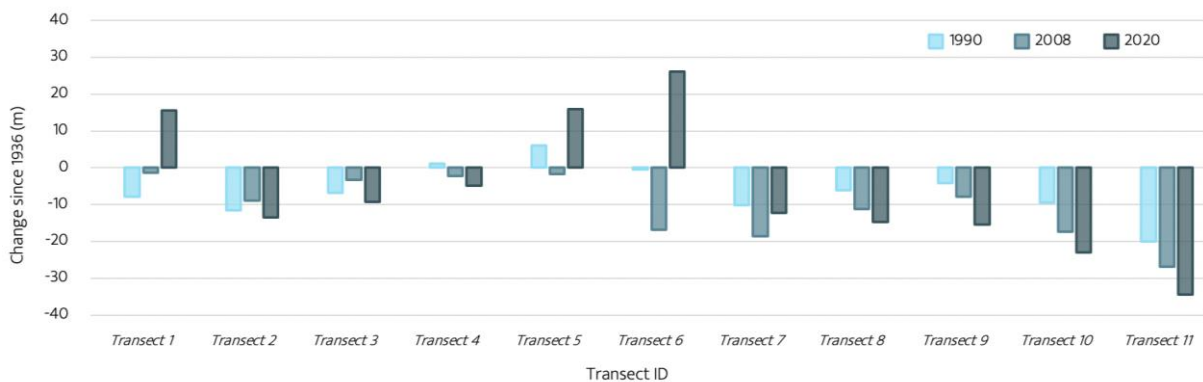


Figure 13 - Staple diagram with the variation along the coastline, 1990, 2008 and 2020 compared to 1936. A negative value indicates degradation while a positive change indicates advancement of the coastline.

Source: Authors own (2022).

Figur 13 - Stapeldiagram med variationen längst kustlinjen 1990, 2008 och 2020 jämfört med 1936. Ett negativt värde indikerar tillbakagång, medans en positiv förändring indikerar tillväxt av kustlinjen.

Källa: Författarnas egna (2022).

## 5.2 Glacial change

When examining the glacial development of Brandtbreen since 1936 a retreat has taken place, figure 14. It is noticeable by looking at the terminal moraine that in 1936 the glacial snout was approximately at maximum extent, although it is not possible to determine how the moraine was formed through remote sensing. As of 2020 only a small part of Brandtbreen is still located in Hanaskogdalen.

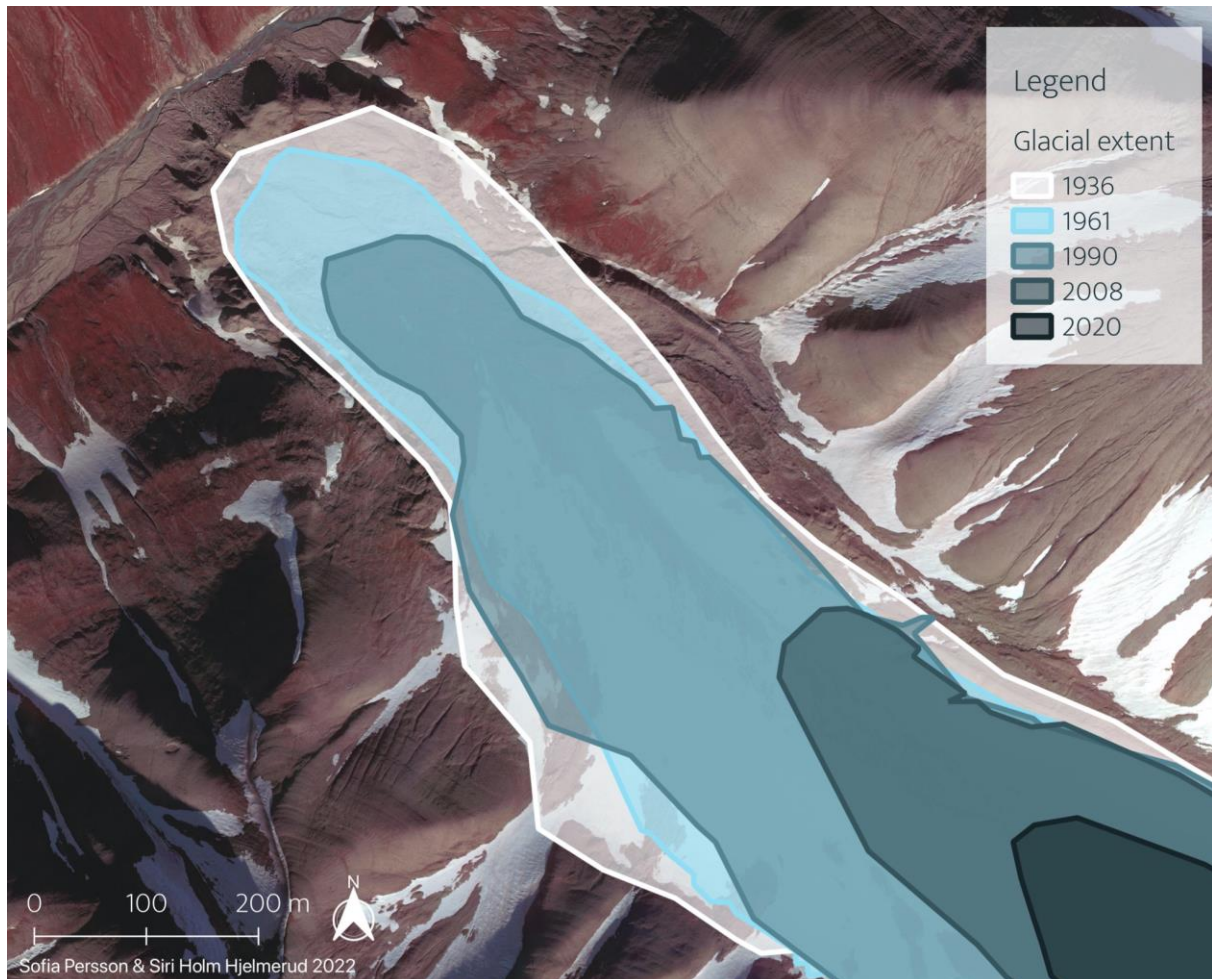


Figure 14 - Glacial extent of Brandtbreen in 1936, 1961, 1990, 2008 and 2020.

Source: Authors own (2022). Data source: DLR, NPI & Geyman et al. (2021) (EPSG:3995).

Figur 14 - Glacial utbredning av Brandtbreen år 1936, 1961, 1990, 2008 och 2020.

Källa: Författarens egna (2022). Datakälla: DLR, NPI & Geyman et al. (2021) (EPSG:3995).

The glacial snout in Hanaskogdalen has decreased from ~29,5 ha in 1936 to ~1,8 ha in 2020, a decline of ~27,7 ha, figure 15. From 1936 to 1990 the ablation of the glacier was approximately 10 ha. The most distinct retreat of the glacier appears between 1990 and 2008, from ~19,6 to ~7,2 ha, even though this is not the longest timespan.

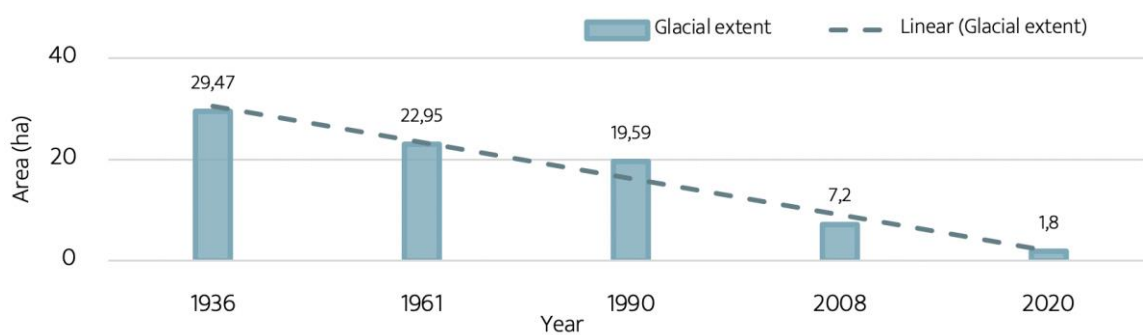


Figure 15 - Diagram of the ablation of Brandtbreen in hectares, including the linear trendline.

Source: Authors own (2022).

Figur 15 - Diagram av ablationen av Brandtbreen i hektar, inkluderat den linjära trendlinjen.

Källa: Författarnas egna (2022).

### 5.3 Climate change

During the studied period (1976-2020) there has been an increase both concerning mean annual air temperature and total annual precipitation, figure 16. Regarding temperature change there is a fluctuation between years. Since 1976 the highest measured mean annual air temperature was in 2016 at  $-0.1^{\circ}\text{C}$ , while the lowest was recorded in 1988 at  $-8.9^{\circ}\text{C}$ . Comparing the first and last ten years of the period, the first (1976-1985) had only one year with a mean annual air temperature over  $-4^{\circ}\text{C}$  (1984) while in the last period (2011-2020) the annual mean did exceed  $-4^{\circ}\text{C}$  every year. Considering precipitation, a variation can be detected as well. The highest amount of yearly precipitation was measured in 2016 (310 mm) and the lowest in 1998 (91,9 mm). During the first ten years in the time series (1976-1985) there were four years not exceeding 150 mm/year (1977, 1978, 1982 & 1983) while during the last ten years measured (2011-2020) there was one (2020).

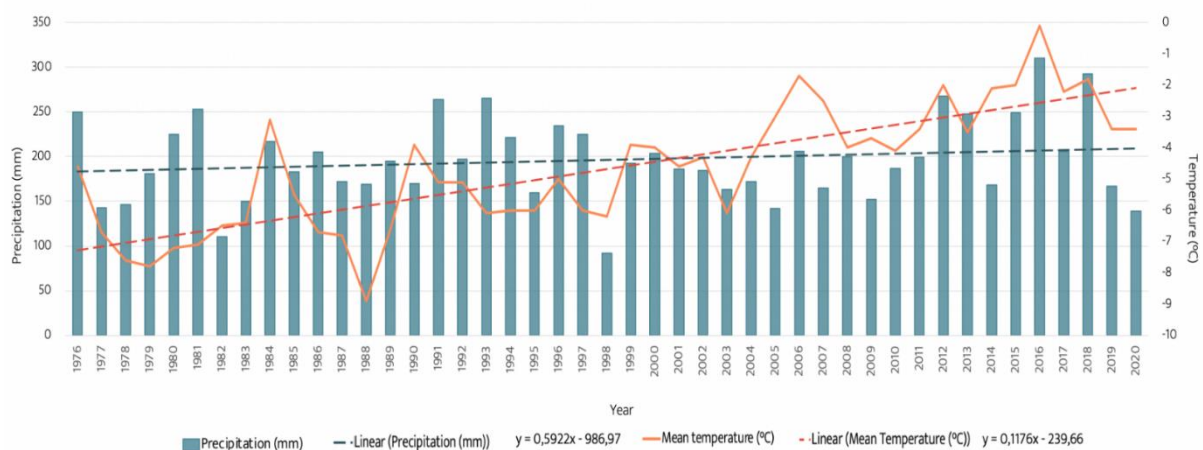


Figure 16 - Mean annual air temperature and total annual precipitation at SN99840 between 1976 and 2020, including linear trends. Source: Authors own (2022). Data source: Norsk Klimaservicesenter.

Figur 16 - Årlig medel lufttemperatur och total årlig nederbörd vid SN99840 mellan 1976 och 2020, inkluderat linjära trender. Källa: Författarnas egna (2022). Datakälla: Norsk Klimaservicesenter.

Looking at summer precipitation, figure 17, there is also a positive trend. Some fluctuation in the amount of precipitation can be detected throughout the period. It is noticeable that 2013 stands out with the largest amount (136 mm) and 1998 with the lowest (18,1 mm). Between 1976 and 1985 three years had summer precipitation over 60 mm/year (1976, 1980 & 1981) compared to six years during the period of 2011-2020 (2012, 2013, 2015, 2016, 2018 & 2019).

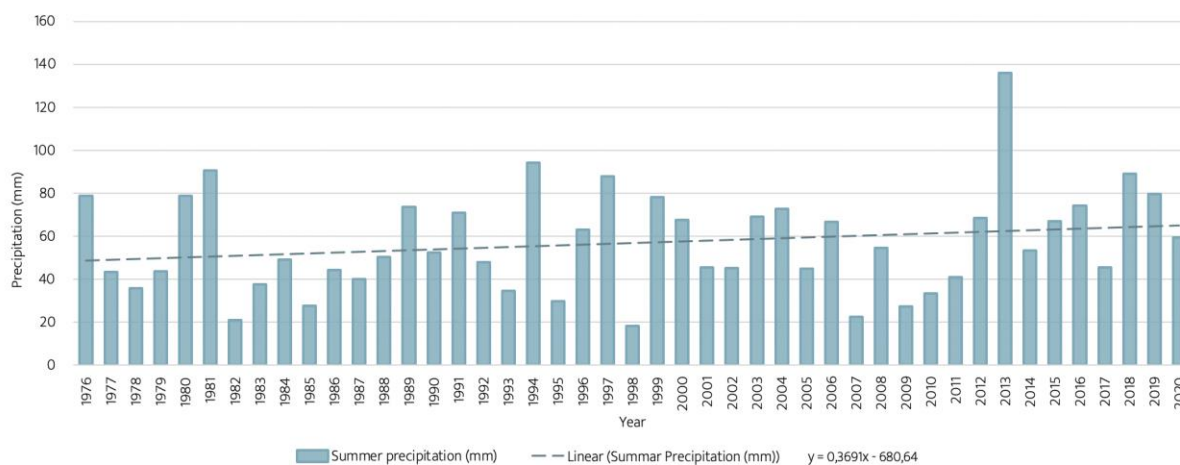


Figure 17 - The yearly variation of summer precipitation (precipitation fallen between 15<sup>th</sup> June and 15<sup>th</sup> of September on days when minimum temperature is over 0°C) at SN99840. Source: Authors own (2022). Data source: Norsk Klimaservicesenter.

Figur 17 - Den årliga variationen av sommarregn (nederbörd mellan 15:e juni och 15:e september på dagar när minimumtemperaturen är över 0°C) vid SN99840. Källa: Författarnas egna (2022). Datakälla: Norsk Klimaservicesenter.

Regarding days with heavy precipitation a positive trend can be detected, figure 18. The graph displays high values in 1994 (7 days), 1996 (7 days) and 2013 (11 days). Additionally, no days with heavy rain, according to the definition of this study, were detected in 1982, 2007, 2010 and 2011. Comparing the number of years with a minimum of four days with heavy precipitation between the first and the last ten year period during the studied timespan, there are two years between 1976 and 1985 (1980 & 1981) and seven between 2011 and 2020 (2012, 2013, 2015, 2016, 2018, 2019 & 2020).

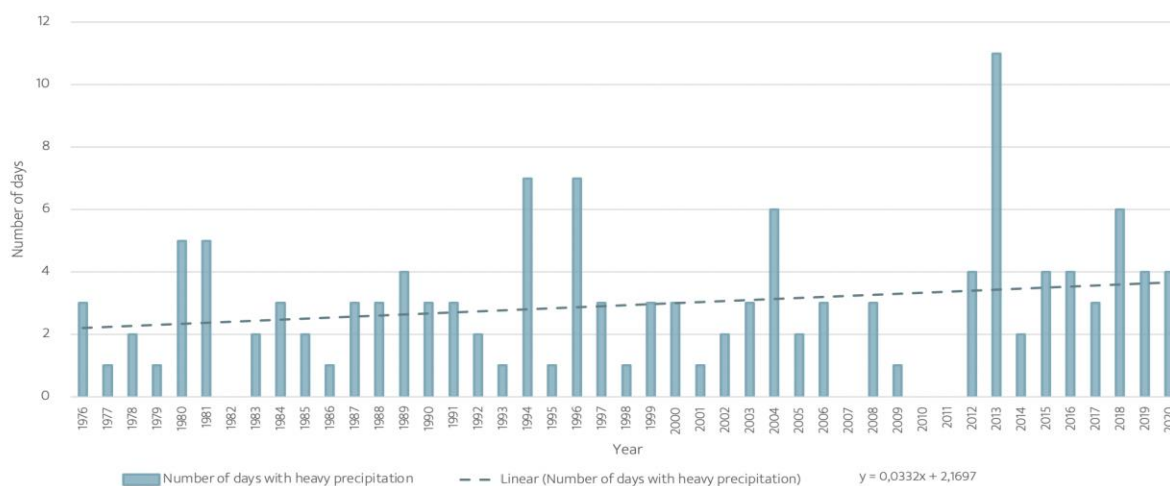


Figure 18 - The total number of days with heavy precipitation (>5 mm/day that has fallen between 15th June and 15th of September on days when minimum temperature is over 0°C) between 1976 and 2020.

Source: Authors own (2022). Data source: Norsk Klimaservicesenter.

Figur 18 - Antal dagar med kraftig nederbörd (>5mm/dag mellan 15 juni och 15 september när minimum temperaturen är över 0°C) mellan 1976 och 2020.

Källa: Författarens egna (2022). Datakälla: Norsk Klimaservicesenter.

Concerning the changed local climate the chosen variables have all experienced a positive trend since 1976, see table 2. This implies that there has been an increase in mean annual air temperature, total annual precipitation, summer precipitation and days with heavy precipitation. However, the correlation is not statistically significant for the variables except for the temperature change. Regarding the increased mean annual air temperature there is a strong correlation and the  $\beta$ -coefficient indicates that for every year the temperature increases on average  $\sim 0.12^\circ\text{C}$ . When comparing the precipitation variables it is notable that total annual precipitation is the variable with the highest  $\beta$ -coefficient implying the biggest average increase since 1976 ( $\sim 0.6\text{mm /year}$ ). However, since the  $p$ -value is not below 0.05 the change is not statistically significant. Table 2 additionally includes  $R^2$  for the variables. Mean annual air temperature has the highest  $R^2$  value,  $\sim 62\%$  of the temperature change is explained by the independent variable (time).

*Table 2 - Trends and significance looking at the different dependent climate variables in relation to the independent variable time (years). The  $\beta$ -coefficient is displayed in the table's first row under the dependent variables, followed by its  $t$ -value. Additionally, including the intercept with the  $t$ -value as well as number of observations ( $N$ ) and  $R^2$  value. Source: Authors own (2022).*

*Tabell 2 - Trender och signifikans för de valda, beroende, klimatvariablerna i relation till den oberoende variabeln tid (år).  $\beta$ -koefficienten visas på tabellens första rad under de beroende variablerna följt av dess  $t$ -värde. Vidare inkluderas interceptet med dess  $t$ -värde och antalet observationer ( $N$ ) och  $R^2$  värdet. Källa: Författarnas egna (2022).*

	(1)	(2)	(3)	(4)
	Mean temperature	Annual precipitation	Summer precipitation	Days with heavy precipitation
Year	0.118*** (8.39)	0.592 (1.11)	0.369 (1.38)	0.032 (1.36)
Intercept	-239.7*** (-8.56)	-987.0 (-0.93)	-680.6 (-1.27)	-63.40 (-1.30)
$N$	45	45	45	45
$R^2$	0.621	0.028	0.042	0.041

*t* statistics in parentheses

\*  $p < 0.05$ , \*\*  $p < 0.01$ , \*\*\*  $p < 0.001$

## 6. Discussion

The result shows an increase in geomorphological activity considering debris flows, fluvial activity, accumulation of sediment and erosion in Hanaskogdalen. The number of debris flows has increased both when comparing actual and relative numbers. The accelerating geomorphological activity in Hanaskogdalen is confirming the result of previous studies stating that more debris flows are appearing (Bernhardt et al., 2017). New debris flows per year have increased to approximately four between 2008 and 2020. There is also an increase when comparing the two earlier periods, however the 1961 data did not cover the entire valley and therefore there may be an underestimation between 1961 and 1990. Nevertheless, the missing data is over the western part of the valley, while most of the new debris flows have been observed on the larger alluvial fans in the eastern part. It is therefore possible to draw the conclusion that the majority of the new debris flows have been detected. Considering these factors a reliable comparison can be done between 1990-2008 and 2008-2020 since the data is of good quality and covers the entire valley, showing a distinct change from  $\sim 0,78/\text{year}$  to  $\sim 4/\text{year}$ . The development can be discussed in relation to precipitation change since rainfall on a snow free ground in general, and intense rainfall in particular, is a triggering factor for Arctic debris flows (Bernhardt et al., 2017). This study shows that an increase in total precipitation, summer precipitation and days with heavy precipitation have appeared simultaneously as the increase of new debris flows. Although it is important to remember that none of the precipitation trends are statistically significant. Furthermore, one can discuss the possible future changes. The increased mean annual air temperature in the area is statistically significant, and it has the ability to accelerate permafrost thawing leading to a thicker active layer. This could cause a higher threshold of water needed to saturate the ground which is a triggering factor for debris flows (French, 2007, p. 233; Mason et al., 2016, p. 556). Considering this, there is a possibility that less new debris flows would occur if the increased precipitation is at a lower speed than increased air temperature.

The result shows a change in the coastline since 1936 both regarding erosion and accumulation of sediment. Generally, there is erosion along the coastline at various degrees which could be caused by different aspects. With a higher sea level new surfaces are exposed to frost weathering, thermal erosion and wave action which can accelerate erosion (Ballantyne & Harris, 1994, p. 267; Dupeyrat et al., 2011). Accumulation of sediment along the coastline has appeared in two periods, between 1936-1990 and 2008-2020, near the river outlet. Between

1936 and 1990 the area around the river mouth was subjected to accumulation as well as degradation, however the poorer detail in the 1936-data entails a risk of misinterpretation. On the other hand the accumulation of sediment between 2008 and 2020 is clearly visible, and the landform can be interpreted as a delta (Mason et al., 2016, p. 504-506). As presented in the *knowledge overview* section of this paper, delta formation is regulated by the amount of sediment which in turn is regulated by the amount of water (Beylich & Gintz, 2004). The development of the delta during the last 12 years (2008-2020) indicates a change in sediment transport, possibly caused by an increased amount of runoff. The increased rainfall, both considering summer precipitation and days with heavy precipitation, could possibly contribute to a larger amount of runoff. However, due to a small number of regression analysis points causalities between the changes could not be established even if they occur simultaneously. Furthermore, the changed temperature can influence the formation of the coastline since the increased mean annual air temperature can accelerate the thawing of permafrost, leading to a bigger amount of unfrozen sediment that could be transported to the coastline. Regarding erosion, the increased temperature can affect the coastline variations as well because it is the main factor contributing to a higher sea level (NASA, 2022). It is worth mentioning that variables not regarded by this study, such as currents and tides, also influences the formation of a delta (Mason et al., 2016, p. 504).

Concerning the glacial snout of Brandtbreen located in Hanaskogdalen the result shows that the area covered by the glacier has decreased between 1936 and 2020. From 1990 to 2008 the largest cutback was detected (from ~19,6 ha to ~7,2 ha) although this is not the longest timespan. This corresponds with global patterns that glaciers are melting at accelerating speed (WGMS, 2021) and the declining trend indicates a negative mass balance. As earlier mentioned this can be caused either by a lower accumulation or a more extensive ablation (Mason et al., 2016, p. 524-525). The climate analysis states that there is an increase in annual precipitation as well as a significant temperature increase. A higher amount of annual precipitation is not equal to accumulation of the glacier, especially since the other precipitation variables show a positive trend indicating an increased amount of rain. The decrease of Brandtbreen observed by this study gives indication that the temperature increase has a larger effect on the glacial mass balance than the increased precipitation. This is in line with the fact that the mean annual air temperature change is statistically significant.

The ablation of Brandtbreen can be put in relation to the geomorphological development of the landscape since they appeared simultaneously. The runoff from the melting glacier could add to the saturation of the active layer which can trigger debris flows (French, 2007, p. 233). It is also one of the contributing factors to rising sea levels leading to accelerating coastline erosion (Ballantyne & Harris, 1994, p. 271). Furthermore, the increased runoff could imply elevated sediment transport (Beylich & Gintz, 2004) possibly being a reason for the delta development. The ground in areas previously covered by the glacier are more prone to geomorphological activity (de Haas et al., 2015) which may be a contributing factor to the larger amount of sediment, affecting delta development. This paper observed multiple changes in the landscape between 1936 and 2020, however it could be of interest to further investigate the appearance of different landforms such as molarids which could be used as indicators for permafrost thawing (Morino et al., 2019).

All studied climate variables show a positive trend indicating an increase of mean annual air temperature, annual precipitation, summer precipitation and days with heavy precipitation in Hanaskogdalen. The only statistically significant change that could be established was the change in mean annual air temperature, which is in line with global patterns (IPCC, 2018b). Considering the precipitation variables, no significance can be found between 1976 and 2020. However, all trends are positive and are not in contrast to global patterns (ibid). As earlier mentioned, different studies have gotten different results regarding significance in climate variables in Svalbard (Bernhardt et al., 2017; Førland & Hanssen-Bauer, 2003; Hanssen-Bauer, 2002; Hanssen-Bauer & Førland, 1998; Jörpeland, 2014). A reason for this could be the various time spans studied. A prolonged timespan could possibly alter the results considering significance. It is important to take into account the fact that this study is limited to four climate variables, possibly excluding others that could have been of interest. A climate analysis including more variables could give a broadened understanding of the local climate.

### ***6.1 Impacts on society***

Drawing on the result of this study it can be established that the people living in Svalbard, particularly in Longyearbyen, already have experienced a changed mean annual air temperature, annual precipitation, summer precipitation and number of days with heavy precipitation since 1976. In the nearby region there is an increase of geomorphological activity considering debris flows, a changed coastline as well as an ablation of Brandtbreen. This result

is in agreement with previous studies showing that life in Longyearbyen already is altered due to climate change (Timlin et al., 2022), and seeing to the result of this study the physical variations in the nearby landscapes can not be expected to decrease in the future. The increased mass movements and changed coastline detected in Hanaskogdalen can indicate that the same changes are to be expected in Longyearbyen, which could have an extensive effect on infrastructure and everyday life (Mason et al., 2016, p. 556). For example, debris flows happening in built-up areas could destroy houses or roads. On a broader scale, the consequences for the Earth's climate system connected to possible feedback processes also must be discussed. The temperature rise and the increased occurrence of debris flows can indicate a declining permafrost table that can limit the natural carbon sequestration, resulting in less carbon being held in the soil and more emitted into the atmosphere (Masyagina et al., 2019). This can also be affected by the level of summer precipitation since it regulates soil moisture and aerobic conditions in the soil cause more extensive emissions (Song et al., 2020). The ablation of Brandtbreen is a part of the ice-albedo feedback and the reflection of solar radiation is limited due to loss of ice. A decline of ocean-ice can lead to an increased amount of warm air to pass up over land, possibly resulting in accelerating snowmelt that could further limit the reflectance of the surface (Norwegian Meteorological Institute, 2021). Today, the net radiative heat is limited by the snow reflecting radiation. An accelerated melting of snow and ice possibly limits this, which could create more net radiative heat for the region during the period of continuous daylight. To further understand the local changes in the area a field study could provide further depth and insights of the landscape. Since this study was conducted during spring which inhibited adequate geomorphological observations in the field a future interest could be to complement it with an in situ study.

## **7. Conclusion**

To conclude, this study has detected multiple physical changes in Hanaskogdalen, Svalbard over the last decades. Concerning geomorphological and glacial change, variations regarding debris flows, fluvial activity, accumulation of sediment, erosion and glacial ablation are visual when comparing aerial photos from 1936, 1961, 1990, 2008 and 2020. There is an increase of geomorphological activity considering debris flows, development of the coastline and an acceleration of glacial degradation throughout the studied period. This could possibly be explained by the detail in the data, however when comparing the two most recent periods (1990-2008 and 2008-2020), in which the data is of high resolution, there is still a distinct elevation of observable changes. Regarding local climate, temperature and precipitation have changed in the area between 1976 and 2020. All studied variables show a positive trend, however only the mean annual air temperature increase is statistically significant. The geomorphological and glacial changes are occurring simultaneously with the altered local climate, however a causality can not be established through statistical analysis.

For people living in close proximity to Hanaskogdalen and other societies in similar environments this study is of relevance because the results are indicating accelerating mass movements and a changed local climate. Connecting this case study with the Earth's climate system gives a larger perspective and an insight on the complexity of changing landscapes, and how all changes are interacting with and have the possibility to affect one another.

## 8. References

Anisimov, O.A., Vaughan, D. G., Callaghan, T. V., Furgal, C., Marchant, H., Prowse, T. D., Vilhjálmsson, H. & Walsh, J. E. (2007). Polar regions (Arctic and Antarctic). *IPCC*.

Retrieved from: <https://www.ipcc.ch/site/assets/uploads/2018/02/ar4-wg2-chapter15-1.pdf>

Ballantyne, C. K. & Harris, C. (1994). *The periglaciation of Great Britain*. Cambridge: Cambridge University Press.

Bernhardt, H., Reiss, D., Heisinger, H., Hauber, E. & Johnsson, A. (2017). Debris flow recurrence periods and multi-temporal observations of alluvial fan evolution in central Spitsbergen Svalbard. *Geomorphology*, 296, 132-141. doi:

<https://doi.org/10.1016/j.geomorph.2017.08.049>

Beylich, A. A. & Gintz, D. (2004). Effects of high-magnitude/low-frequency fluvial events generated by intense snowmelt or heavy rainfall in arctic periglacial environments in northern Swedish lapland and northern Siberia. *Geografiska Annaler: Series A, Physical Geography*, 86:1, 11-29. doi: <https://doi.org/10.1111/j.0435-3676.2004.00210.x>

Climate change & infectious diseases group. (2019). World map of the Köppen-Geiger climate classification updated. *Climate change & infectious diseases group*. Retrieved from:

<http://koeppen-geiger.vu-wien.ac.at/present.htm>

Cortinhas, C., & Black, K. (2012). *Statistics for business and economics*. Chichester: Wiley.

de Haas, T., Kleinhans, M. G., Carbonneau, P. E., Rubensdotter, L. & Hauber, E. (2015). Surface morphology of fans in the high-Arctic periglacial environment of Svalbard: Controls and processes. *Earth-Science reviews*, 146, 163-182.

doi: <https://doi.org/10.1016/j.earscirev.2015.04.004>

Deutsches Zentrum für Luft- und Raumfahrt (2010). HRSC-AX flight campaign. *DLR*.

Retrieved from: [http://europlanet.dlr.de/Svalbard/HRSC\\_AX.html](http://europlanet.dlr.de/Svalbard/HRSC_AX.html)

Deutsches Zentrum für Luft- und Raumfahrt (n.d.). MACS-Polar. *DLR*. Retrieved from:  
[https://www.dlr.de/os/en/desktopdefault.aspx/tabid-12968/22666\\_read-52502/](https://www.dlr.de/os/en/desktopdefault.aspx/tabid-12968/22666_read-52502/)

Dupeyrat, L., Costard, F., Randriamazaoro, R., Gailhardis, E., Gautier, E. & Fedorov, A. (2011). Effects of ice content on the thermal erosion of permafrost: Implications for coastal and fluvial erosion. *Permafrost and periglacial processes*, 22:2, 179-187. doi:  
<https://doi.org/10.1002/ppp.722>

European Space Agency (n.d.). Optical properties of ice and snow. *Eduspace*. Retrieved from:  
[https://www.esa.int/SPECIALS/Eduspace\\_Global\\_EN/SEMPJ7TWLUG\\_0.html](https://www.esa.int/SPECIALS/Eduspace_Global_EN/SEMPJ7TWLUG_0.html)

French H. M. (2007). *The Periglacial Environment*. West Sussex: John Wiley & Sons Ltd.

Førland, E. J. & Hanssen-Bauer, I. (2003). Past and future climate variations in the Norwegian Arctic: Overview and novel analysis. *Polar research*, 22:2, 113-124. doi:  
<https://doi.org/10.3402/polar.v22i2.6450>

Geyman, E., van Pelt, W., Maloof, A., Aas, H. F. & Kohler, J. (2021). Supplementary data for: “Historical glacier change on Svalbard predicts doubling of mass loss by 2100”. *Zenodo*. Retrieved from: <https://zenodo.org/record/5806388#.YI0vEOgza5e>

Guerra, A. J. T., Fullen, M. A., Jorge, M. C. O., Bezerra, J. F. R. & Shokr, M. S. (2017). Slope processes, mass movement and soil erosion: A review. *Pedoshpere*, 27:1, 27-41. doi:  
[https://doi.org/10.1016/S1002-0160\(17\)60294-7](https://doi.org/10.1016/S1002-0160(17)60294-7)

Hanssen-Bauer, I. (2002). Temperature and precipitation in Svalbard 1912–2050: Measurements and scenarios. *Polar Record*, 38:206, 225-232.  
doi: 10.1017/S0032247400017757

Hanssen-Bauer, I. & Førland, E. J. (1998). Long-term trends in precipitation and temperature in the Norwegian Arctic: Can they be explained by changes in atmospheric circulation patterns? *Climate research*, 10:2, 143-153. Retrieved from:  
<https://www.jstor.org/stable/24865962>

Harrie, L. (2013). *Geografisk informationsbehandling: Teori, metoder och tillämpningar*. Lund: Studentlitteratur.

Hauber, E., Reiss, D., Ulrich, M., Preusker, F., Trauthan, F., Zanetti, M., Heisinger, H., Jaumann, R., Johansson, L., Johnsson, A., Olvmo, M., Carlsson, E., Johansson, H. A. B. & McDaniel, S. (2011). Periglacial landscapes on Svalbard: Terrestrial analogs for cold-climate landforms on Mars. *The Geological Society of America*, 483, 177-201.  
doi: 10.1130/2011.2483(12)

Howard, H. R., Manandhar, S., Wang, Q., Mcmillan, J. M., Qie, G., Liu, X., Thapa, K., Xu, X. & Wang, G. (2022). Spatially characterizing land surface deformation and permafrost active layer thickness for Donnelly installation of Alaska using DInSAR and MODIS data. *Cold regions science and technology*, 196. doi:  
<https://doi.org/10.1016/j.coldregions.2022.103510>

Intergovernmental Panel of Climate Change (2018a). Summary for Policymakers. In V. Masson-Delmotte, P. Zhai, H.-O. Pörtner, D. Roberts, J. Skea, P.R. Shukla, A. Pirani, W. Moufouma-Okia, C. Péan, R. Pidcock, S. Connors, J.B.R. Matthews, Y. Chen, X. Zhou, M.I. Gomis, E. Lonnoy, T. Maycock, M. Tignor, and T. Waterfield (eds.), *Global Warming of 1.5°C. An IPCC Special Report on the impacts of global warming of 1.5°C above pre-industrial levels and related global greenhouse gas emission pathways, in the context of strengthening the global response to the threat of climate change, sustainable development, and efforts to eradicate poverty*, (pp. 32). Retrieved from:  
<https://www.ipcc.ch/sr15/chapter/spm/>

Intergovernmental Panel of Climate Change (2018b). Impact of 1.5°C global warming on natural and human systems. In Hoegh-Guldberg, O., Jacob, D., Taylor, M., Bindi, M., Brown, S., Camilloni, I., Diedhiou, A., Djalante, R., Ebi, K.L., Engelbrecht, F., Guiot, J., Hijioka, Y., Mehrotra, S., Payne, A., Seneviratne, S.I., Thomas, A., Warren, R. & Zhou, G. (eds.), *Global Warming of 1.5°C. An IPCC Special Report on the impacts of global warming of 1.5°C above pre-industrial levels and related global greenhouse gas emission pathways, in the context of strengthening the global response to the threat of climate change, sustainable development, and efforts to eradicate poverty*. Retrieved from: <https://www.ipcc.ch/sr15/chapter/chapter-3/>

Jones, H. G. & Vaughan, R. A. (2010). *Remote sensing of vegetation: Principles, techniques and applications*. Oxford: Oxford University Press.

Jörpeland, J. (2014). *Analysis of temperature and precipitation trends at Svalbard 1989-2010*. (Självständigt arbete nr. 112). Uppsala: Uppsala University. Retrieved from: <https://www.diva-portal.org/smash/get/diva2:772298/FULLTEXT02>

Mason, J. A., Burt, J. E., Muller, P. O. & de Blij, H. J. (2016). *Physical geography: The global environment*. New York: Oxford University Press.

Masyagina, O. V., Evgrafova, S. Y., Bugaenko, T. N., Kholodilova, V. V., Krivobokov, L. V., Korets, M. A. & Wagner, D. (2019). Permafrost landslides promote soil CO<sub>2</sub> emission and hinder C accumulation. *Science of the total environment*, 657, 351-364. doi: <https://doi.org/10.1016/j.scitotenv.2018.11.468>

McCann, S. B., Howarth, P. J. & Cogley, J. G. (1972). Fluvial processes in a periglacial environment. *Transactions of the Institute of British Geographers*, 55, 69-82. doi: <https://doi.org/10.2307/621723>

Morino, C., Conway, S. J., Sæmundsson, Þ., Helgason, J. K., Hillier, J., Butcher, F. E. G., Balme, M. R., Jordan, C. & Argles, T. (2019). Molards as an indicator of permafrost degradation and landslide processes. *Earth and Planetary science letters*, 516, 136-147. doi: <https://doi.org/10.1016/j.epsl.2019.03.040>

National Aeronautics and Space Administration (2022). Sea level. NASA. Retrieved from: <https://climate.nasa.gov/vital-signs/sea-level/>

National Snow & Ice Data Center. (2020). How do glaciers affect land? NSIDC. Retrieved from: <https://nsidc.org/cryosphere/glaciers/questions/land.html>

Norsk Klimaservicesenter (n.d.). Seklima: Observasjoner og værstatistikk. Norsk Klimaservicesenter. Retrieved from: <https://seklima.met.no/observations/>

Norwegian Meteorological Institute (n.d.). Janssonhaugen, Svalbard (275 m a.s.l.). *Cryo*.

Retrieved from: <https://cryo.met.no/index.php/en/permafrost/janssonhaugen>

Norwegian Meteorological Institute (2021). Svalbard: Trends in snow cover and sea-ice area.

*Cryo*. Retrieved from: <https://cryo.met.no/en/svalbard-cryosphere-sess>

Sollid, J. L. & Christiansen, H. H. (Eds.) (2003). *Permafrost, periglacial features and glaciers in Svalbard: Field excursion guide*. VIII. International Conference on Permafrost.

Rapportserie i naturgeografi, Universitetet i Oslo. Rapport nr. 14, 145 pp.

Song, X., Wang, G., Ran, F., Huang, K., Sun, J. & Song, C. (2020). Soil moisture as a key factor in carbon release from thawing permafrost in a boreal forest. *Geoderma*, 357. doi:

<https://doi.org/10.1016/j.geoderma.2019.113975>

Steffen, W., Rockström, J., Richardson, K. & Schellnhuber, H. J. (2018) Trajectories of the Earth system in the anthropocene. *Proceedings of the national academy of sciences*, 115:33.

doi: <https://doi.org/10.1073/pnas.1810141115>

Tananaev, N. & Lotsari, E. (2022). Defrosting northern catchments: Fluvial effects of permafrost degradation. *Earth-Science reviews*, 228. doi:

<https://doi.org/10.1016/j.earscirev.2022.103996>

Thuesen, N. P. & Barr, S. (2022). Svalbard. *Store Norske Leksikon*. Retrieved from:

<https://snl.no/Svalbard>

Timlin, U., Meyer, A., Nordström, T. & Rautio, A. (2022). Permafrost thaw challenges and life in Svalbard. *Current research in environmental sustainability*, 4. doi:

<https://doi.org/10.1016/j.crsust.2021.100122>

World glacier monitoring service. (2021). Global Glacier Change Bulletin No. 4 (2018-2019).

Zemp, M., Nussbaumer, S. U., Gärtner-Roer, I., Bannwart, J., Paul, F., and Hoelzle, M. (eds.), ISC(WDS)/IUGG(IACS)/UNEP/UNESCO/WMO, World Glacier Monitoring Service,

Zurich, Switzerland, 278 pp., publication based on database version: [doi:10.5904/wgms-fog-2021-05](https://doi.org/10.5904/wgms-fog-2021-05).